Catalysis Science & Technology

PAPER

View Article Online
View Journal | View Issue

Open Access Article. Published on 01 August 2016. Downloaded on 8/2/2025 8:34:17 AM.
This article is licensed under a Creative Commons Attribution-NonCommercial 3.0 Unported Licence.

Cite this: *Catal. Sci. Technol.*, 2016, **6**, 7280

Accessibility enhancement of TS-1-based catalysts for improving the epoxidation of plant oil-derived substrates†

Nicole Wilde,[a] Jan Přech,[b] Marika Pelz,[a] Martin Kubů,[b] Jiří Čejka[b] and Roger Gläser*[a]

Received 6th June 2016,
Accepted 1st August 2016

DOI: 10.1039/c6cy01232a

www.rsc.org/catalysis

TS-1-based catalysts with different textural features, namely layered TS-1, pillared TS-1, and Ti-pillared TS-1 as well as mesoporous TS-1, were investigated in the liquid-phase epoxidation of methyl oleate as a model compound for plant oil-derived substrates with hydrogen peroxide at 50 °C. While over the TS-1-based catalysts, except Ti-pillared TS-1, an epoxide selectivity of up to 93% is achieved, layered and pillared TS-1 are the most active (the amounts of methyl oleate converted after 5 h per number of Ti-sites are 4.64 mol mol^{-1} and 4.68 mol mol^{-1}) with an efficiency for H_2O_2 conversion to the epoxide of 27%. Mesoporous TS-1 and conventional microporous TS-1 exhibit a similar activity (3.64 mol mol^{-1} *vs.* 3.37 mol mol^{-1}), whereas the mesoporous catalyst most efficiently utilizes H_2O_2 (39% efficiency). The lowest catalytic activity (0.82 mol mol^{-1}), epoxide selectivity as well as H_2O_2 efficiency are observed over Ti-MCM-36, possessing mainly octahedrally coordinated Ti-sites. The results demonstrate the importance of accessibility of Ti-sites at external crystal surfaces within layered and pillared TS-1, significantly increasing the epoxidation activity with respect to the number of Ti-atoms present in the catalysts.

1. Introduction

Titanium silicalite-1 (TS-1) is a well-known catalyst for the oxidation of organic substrates with aqueous H_2O_2 utilizing isolated Ti(IV)-sites in a hydrophobic, microporous silicalite framework.[1–3] This allows for the simultaneous adsorption of the often hydrophobic substrates and H_2O_2 as a hydrophilic oxidant. Especially for the epoxidation of C=C double bonds, TS-1 is the catalyst of choice for numerous organic substrates.[2–6] Epoxidized plant oils and their derivatives are attractive intermediates for a broad range of large-scale industrial applications as well as precursors to a wide series of value-added compounds such as bio-based epoxy resins, non-isocyanate-based polyurethanes and bio-lubricants.[7–10] It was recently shown that the epoxidation of vegetable oil-based unsaturated fatty acid methyl esters (FAME), such as methyl oleate, can be accomplished over conventional TS-1 with aqueous H_2O_2 as the oxidizing agent.[11] Methyl oleate is derived from oleic acid which is the most abundant component in a large variety of plant oils. In addition, only one C=C double bond is present in methyl oleate making it a suitable model compound for FAME. In the epoxidation of methyl oleate over conventional TS-1, almost complete conversion and epoxide selectivity up to 93% were achieved.[11] However, the conversion of FAME over TS-1 is limited by mass transfer within the catalyst particles, largely due to the limited size of its micropores with respect to the bulky FAME molecules. In addition, a low H_2O_2 efficiency of 18% (defined as the ratio of moles of product formed to moles of H_2O_2 consumed) was observed which poses an essential hurdle for a "green" and economically viable process.

Titanium-containing silicates with enhanced accessibility of the active Ti-sites could overcome the limitations associated with the relatively small pore width of TS-1.[12–14] Layered titanosilicates are particularly attractive catalysts as they possess active tetrahedrally coordinated titanium sites in their crystalline framework and a high external surface area. Ti-sites on the external surface are accessible without

[a] *Institute of Chemical Technology, Universität Leipzig, Linnéstr. 03, 04103 Leipzig, Germany. E-mail: roger.glaeser@uni-leipzig.de*
[b] *J. Heyrovský Institute of Physical Chemistry, Academy of Sciences of the Czech Republic, v.v.i., Dolejškova 3, 182 23 Prague 8, Czech Republic*

† Electronic supplementary information (ESI) available: Details on the synthesis of the catalysts, nitrogen sorption isotherms for meso-TS-1, layered TS-1, pillared TS-1, Ti-pillared TS-1 and Ti-MCM-36, NLDFT pore width distribution for Ti-MCM-36 and Ti-pillared TS-1 in the range from 0.3 to 4.5 nm, and SEM-EDX maps of pillared TS-1, Ti-pillared TS-1 and Ti-MCM-36. Results on catalyst stability towards leaching from experiments using meso-TS-1, layered TS-1, and pillared TS-1 before and after hot filtration of the catalysts. Nitrogen sorption isotherms, textural properties, powder X-ray diffraction patterns, DR-UV-vis spectra and SEM images of the fresh and regenerated catalysts meso-TS-1, layered TS-1, and pillared TS-1. Investigation of carbonaceous compounds leading to deactivation of conventional TS-1 as well as a proposed reaction scheme for the formation of the carbonaceous compounds. See DOI: 10.1039/c6cy01232a

 This journal is © The Royal Society of Chemistry 2016

Open Access Article. Published on 01 August 2016. Downloaded on 8/2/2025 8:34:17 AM.
This article is licensed under a Creative Commons Attribution-NonCommercial 3.0 Unported Licence.

diffusion restrictions typical for those in microporous channel systems.[14,15] Corma *et al.*[16,17] incorporated titanium into the lamellar silicate ITQ-6 (**FER** topology). The activity of Ti-ITQ-6 (lamellar, turnover number (TON) = 23) exceeds that of Ti-**FER** (purely microporous, TON = 6) and is similar to that of Ti-**BEA** (purely microporous, TON = 20) in the epoxidation of 1-hexene. Wu *et al.*[18,19] described the preparation of Ti-**MWW** *via* its lamellar precursor (denoted as Ti-MCM-22P). Fan *et al.*[20] prepared Ti-YNU-1 (possessing a crystal structure similar to that of the **MWW**-lamellar precursor) and this material exhibits an enhanced activity in the epoxidation of C5–C8 cycloalkenes compared to the 3-dimensional purely microporous Ti-**MWW** (Ti-**MWW**, n_{Si}/n_{Ti} = 45) and Ti-**BEA** (n_{Si}/n_{Ti} = 35), although it has a molar n_{Si}/n_{Ti} ratio as high as 240 (*e.g.*, TON for cyclohexene epoxidation of 1100 for Ti-YNU-1 *vs.* 50 for 3D-Ti-**MWW**). Kim *et al.*[21] prepared a Ti-MCM-36 catalyst by swelling Ti-MCM-22P layers with a surfactant and supporting the layers (pillaring) with amorphous SiO_2 to keep them apart after calcination. This pillared material exhibits a more than three times higher TON than conventional TS-1 in 1-hexene epoxidation at 45 °C ($TON_{Ti\text{-}MCM\text{-}36}$ = 257, $TON_{TS\text{-}1}$ = 81). Wang *et al.*[22] reported the preparation of interlayer-expanded Ti-IEZ-**MWW**. The TON achieved over this material in the epoxidation of cyclohexene is an order of magnitude higher (TON = 233) compared to that of Ti-**MWW** (TON = 33). Ryoo *et al.*[23] described the preparation of nanosheet TS-1 using a specially designed surfactant as a structure-directing agent $(C_{18}H_{37}\text{–}N^{+}(CH_3)_2\text{–}C_6H_{12}\text{–}N^{+}(CH_3)_2\text{–}C_6H_{13}(OH^{-})_2)$[24] instead of the conventionally applied tetrapropylammonium hydroxide. Nanosheet TS-1 exhibits an order of magnitude higher conversion in the epoxidation of cyclohexene and cyclooctene in comparison with conventional TS-1 (cyclooctene conversion: nanosheet TS-1, 15.3% *vs.* TS-1, 0.6% at 60 °C after 2 h). Recently, Přech *et al.*[25] reported a procedure for the pillaring of TS-1 nanosheets. To suppress the active phase dilution, titanium was added also during the pillaring treatment. The resulting Ti-pillared TS-1 is active in cyclooctene and norbornene epoxidation at 60 °C. The yield of cyclooctene oxide over the Ti-pillared TS-1 catalyst (16.9% after 4 h) is increased substantially in comparison with that over pillared TS-1 without titanium addition (yield 3.5%).

An alternative approach to improve the catalytic activity of TS-1 crystals for the epoxidation of substrates with large molecules is to increase the accessibility of the Ti-sites by creating mesopores in the zeolitic framework, *e.g.*, by the preparation of hierarchically structured TS-1 (possessing micro- and mesopores) *via* secondary templating. Jacobsen *et al.*[26] reported the synthesis of mesoporous TS-1 using carbon black pearls. The application of mesoporous TS-1 resulted in the same yield as conventional TS-1 in the epoxidation of 1-octene (ratio between product yield over mesoporous and conventional catalyst after the same reaction time $Y_{mesoporous}/Y_{conventional}$ = 1). However, a 10 times higher yield of cyclohexene oxide ($Y_{mesoporous}/Y_{conventional}$ = 9.5 after 70 min of reaction) was obtained in the epoxidation of cyclohexene with H_2O_2.[26]

In the present study, TS-1-based catalysts with different textural features, *i.e.*, layered TS-1, pillared and Ti-pillared TS-1 as well as mesoporous TS-1, were prepared, thoroughly characterized and investigated in the liquid-phase epoxidation of methyl oleate with H_2O_2 at a mild temperature of 50 °C. The catalytic results achieved over the TS-1-based catalysts are compared to those obtained over a conventional, microporous TS-1 and Ti-MCM-36. It was of particular interest to study, if the catalytic activity of the materials can be enhanced through improving the accessibility of the active Ti-sites by providing porosity in addition to the micropores of conventional TS-1. Fig. 1 shows a schematic comparison of the different catalyst pore structures. In addition to the activity and selectivity, the H_2O_2 efficiency with respect to the structural features of the materials as well as the reusability and regenerability of the catalysts were investigated.

2. Experimental section

2.1 Synthesis of the catalysts

2.1.1 Synthesis of mesoporous TS-1. Mesoporous titanium silicalite-1 (meso-TS-1) was prepared using carbon black pearls (CBP, diameter 20 nm, Cabot) as a secondary templating agent. The procedure was adapted from Taramasso *et al.*[27] and is described in detail in the ESI† (1.1).

2.1.2 Synthesis of layered TS-1. The synthesis of parent layered TS-1 was carried out according to the procedure reported by Ryoo *et al.*[23] starting from TEOS and TBOTi using a surfactant template $C_{18}H_{37}N^{+}(CH_3)_2C_6H_{12}N^{+}(CH_3)_2C_6H_{13}$ in hydroxide form (abbreviated as $C_{18\text{-}6\text{-}6}$), prepared as described in ref. 23. Details are given in the ESI† (1.2).

2.1.3 Pillaring of layered TS-1. The catalysts pillared TS-1 and Ti-pillared TS-1 were prepared from the as-synthesized layered TS-1. No swelling of the material was necessary as the layers are kept apart intrinsically by the surfactant template. The pillaring was performed as described by Přech *et al.*[25] TEOS (for pillared TS-1) and a mixture of TEOS and TBOTi with a n_{Si}/n_{Ti} ratio of 20 (for Ti-pillared TS-1) were mixed with

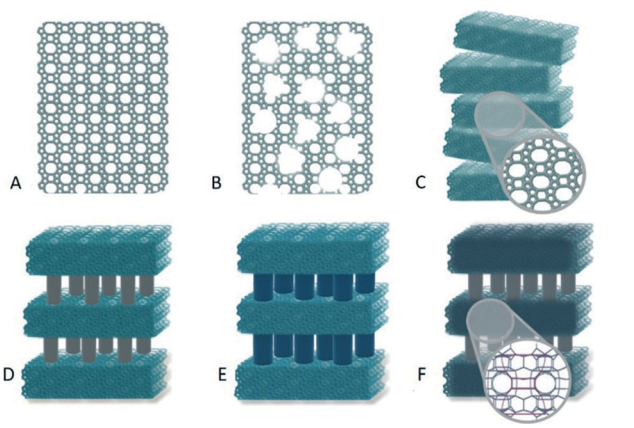

Fig. 1 Schematic representation of the structure of the studied catalysts: conventional TS-1 (A), mesoporous TS-1 (meso-TS-1) (B), layered TS-1 (C), pillared TS-1 (D), Ti-pillared TS-1 (E), and Ti-MCM-36 (F).

Open Access Article. Published on 01 August 2016. Downloaded on 8/2/2025 8:34:17 AM.
This article is licensed under a Creative Commons Attribution-NonCommercial 3.0 Unported Licence.

the as-synthesized layered zeolite (10 g of the TEOS mixture per 1 g of layered TS-1) and stirred at 65 °C for 24 h. Then, the solid was removed by centrifugation and dried for 48 h at room temperature. Subsequently, the product was hydrolyzed in distilled water with 5 wt% ethanol (100 cm^3 g^{-1}) at room temperature for 24 h under vigorous stirring. Finally, the solid material was again removed by centrifugation, dried at 65 °C and calcined in an air flow at 550 °C for 10 h using a temperature ramp of 2 °C min^{-1}.

2.1.4 Synthesis of Ti-MCM-36. The synthesis followed the procedure described by Wu *et al.*[19] and consists of four steps as given in detail in the ESI† (1.3). These steps are (i) the preparation of Ti-MCM-22P, (ii) the removal of extra-framework Ti-species from the as-synthesized Ti-MCM-22P, (iii) the transformation of Ti-MCM-22(P) by a surfactant-assisted swelling step to obtain Ti-MCM-22(SW) followed by (iv) pillaring of Ti-MCM-22SW and calcination to obtain Ti-MCM-36.

An industrial titanium silicalite-1 (TS-1, powder, Evonik) was used as a reference.

2.2 Characterization

X-ray powder diffraction (XRD) patterns were collected using a Bruker AXS D8 Advance diffractometer equipped with a graphite monochromator and a position-sensitive detector Våntec-1 using CuKα radiation in Bragg–Brentano geometry. Data were collected in continuous mode over the 2θ range of 1–40° with a step size of 0.00853° and a time per step of 0.25 s.

Nitrogen sorption isotherms were obtained at liquid nitrogen temperature (−196 °C) with a Micromeritics ASAP 2020 volumetric sorption analyzer. Prior to the analysis, the individual samples were outgassed under vacuum (1.33 Pa) at 250 °C overnight. The sorption isotherms were taken in the relative pressure range of p/p_0 from 0.0050 to 0.9990. The specific BET surface area was evaluated using adsorption data in the relative pressure range of p/p_0 from 0.05 to 0.20. The *t*-plot method[28] was applied to determine the specific volume of micropores (V_{micro}) and the specific external surface area (S_{ext}). The adsorbed amount of nitrogen at $p/p_0 = 0.99$ reflects the total specific adsorption capacity (V_{total}). The pore width distribution (PWD) was calculated from the desorption branch of the hysteresis loop using the BJH algorithm[29] with the Halsey equation.

To determine the characteristics of pores smaller than 3 nm, low-pressure argon sorption was performed for selected samples at −186 °C. The pore width distributions were calculated from the argon adsorption isotherms using the non-local density functional theory (NLDFT) model for cylindrical pores in oxides.

Diffuse reflectance UV-vis (DR-UV-vis) absorption spectra were collected using a Perkin-Elmer Lambda 950 spectrometer with a 2 mm quartz tube and a large slit (8 × 16 mm) at room temperature. The data were collected in the wavelength range of 190–800 nm. All samples were analyzed after calcination.

The chemical composition of the materials (expressed hereafter as the n_{Si}/n_{Ti} ratio) was determined by XRF with a Philips PW 1404 spectrometer using the analytical program UniQuant. The samples were mixed with Dentacryl resin (SpofaDental, Czech Republic) as a binder and pressed onto the surface of cellulose pellets prior to the measurement.

Scanning electron microscopy (SEM) images were taken using a FEI Company Nova NanoLab 200 microscope at 5 kV. Prior to the measurement, the samples were sputtered with gold.

2.3 Catalytic experiments

Catalytic experiments were carried out batchwise in the liquid phase in a two-necked round-bottom glass reactor (V = 25 cm^3) equipped with a magnetic stirrer (400 rpm), a septum and a reflux condenser at 50 °C as described previously.[11] Methyl oleate (MO, 97%, Sigma-Aldrich) was used as a substrate, H_2O_2 (35 wt% aqueous solution, Solvay-Wolfen) was used as the oxidant, acetonitrile (99.9%, BDH Prolabo) served as a solvent and chlorobenzene (99.8%, Aldrich) was the internal standard. In a typical experiment, 10 cm^3 of acetonitrile was loaded into the reactor, followed by the addition of the substrate (MO, 90 mg, 0.30 mmol), H_2O_2 (140 mg, 1.50 mmol) and chlorobenzene (67 mg, 0.60 mmol). The reaction was started by addition of the catalyst (150 mg), dried at 120 °C for 5 h in air prior to the experiment. Samples were taken periodically from the reaction mixture, diluted in acetonitrile and analyzed by capillary gas chromatography.[11]

The conversion of methyl oleate was calculated as the ratio of converted and initially present methyl oleate. The selectivity for methyl 9,10-epoxystearate (epoxide, ME) is given as the mass of epoxide formed relative to the converted mass of the substrate methyl oleate. In order to compare the catalysts with respect to the different Ti-contents, the activity per Ti-sites is calculated as the molar amount of methyl oleate converted after 5 h of reaction divided by the molar amount of Ti-atoms present in the catalysts. The H_2O_2 conversion was calculated from the concentration of H_2O_2 in the initial reactant solution and in the product samples as determined by iodometric titration. The H_2O_2 efficiency ($E_{H_2O_2}$) is defined as the ratio of moles of epoxide formed to moles of hydrogen peroxide consumed. The experimental accuracy was within ±2% for the conversion of methyl oleate, ±6% for the conversion of H_2O_2 and ±5% for the epoxide selectivity.

In reusability tests, three consecutive experiments were carried out as described above. After each repetition, the catalyst was filtered off, washed with 20 cm^3 of acetonitrile, dried at room temperature and added to a fresh reaction mixture.

A regeneration experiment followed the reusability tests. For this purpose, the catalyst was removed from the reaction mixture after the third repetition by filtration, washed with 20 cm^3 of acetonitrile, dried at room temperature and calcined in static air at 400 °C for 24 h. The regenerated catalyst was used in another catalytic experiment.

 This journal is © The Royal Society of Chemistry 2016

Open Access Article. Published on 01 August 2016. Downloaded on 8/2/2025 8:34:17 AM.
This article is licensed under a Creative Commons Attribution-NonCommercial 3.0 Unported Licence.

3. Results and discussion

3.1 Catalyst characterization

The XRD patterns of the prepared catalysts are presented in Fig. 2. The XRD pattern of mesoporous TS-1 (meso-TS-1) shows clear evidence of the presence of the MFI structure. The diffraction pattern of layered TS-1 is consistent with that observed by Ryoo *et al.*[23] for nanosheet TS-1. In the low 2θ region, no diffraction line can be observed due to a random orientation of the layers after calcination. On the other hand, for pillared TS-1 and Ti-pillared TS-1, a strong diffraction line is present at $2\theta = 1.7°$. This line characterizes a regular organization of the layers within these pillared materials.

The position of the diffraction line corresponds to a *d*-spacing of 4.5 nm and an interlayer distance of 2.5 nm (the thickness of the TS-1 layer is approximately 2 nm[23]).

The diffraction lines in the XRD patterns of pillared TS-1 and Ti-pillared TS-1 are less intense due to the presence of amorphous pillars in these materials. For Ti-MCM-36, the main feature of the diffraction pattern (Fig. 2) is an intense diffraction line at $2\theta = 2.1°$ (corresponding to a *d*-spacing of 4.2 nm). This line originates from the organized layered character of the pillared titanosilicate similar to that of pillared TS-1.

The scanning electron micrographs (SEM) shown in Fig. 3 reveal flake-like crystals in agglomerates for all the layered materials studied (Fig. 3, B–E). In the case of the pillared materials (Fig. 3, C–E), the agglomerates are partially covered with amorphous material, probably silica from hydrolysis of the excess TEOS used for the pillaring. Mapping by SEM–EDX (energy-dispersive X-ray spectroscopy) shows that Si and Ti are homogeneously distributed over the materials (ESI,† Fig. S3–S5). In the case of meso-TS-1 (Fig. 3, A), crystals of a sponge-like morphology are observed. This morphology results from the presence of mesopores after removal of the secondary template.

The textural properties of the prepared catalysts are listed in Table 1 and the corresponding sorption isotherms are presented in the ESI† (Fig. S1†).

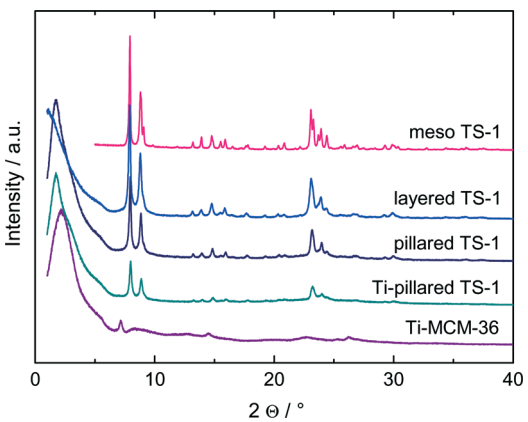

Fig. 2 Powder X-ray diffraction patterns of layered TS-1, pillared TS-1, Ti-pillared TS-1, Ti-MCM-36, and meso-TS-1.

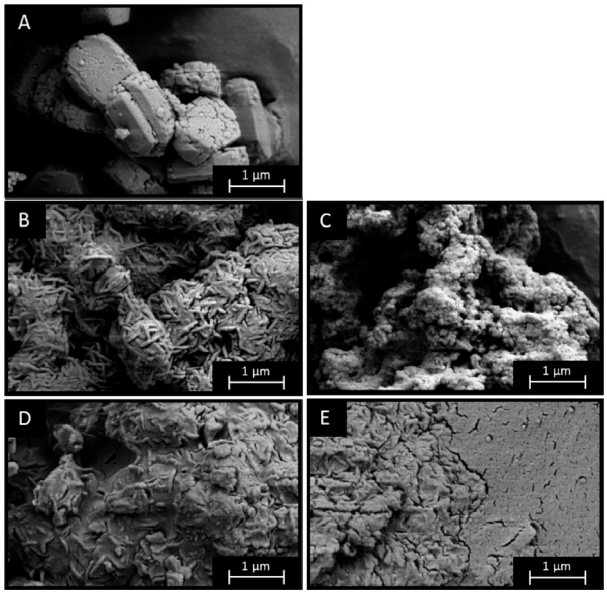

Fig. 3 SEM images of meso-TS-1 (A), layered TS-1 (B), pillared TS-1 (C), Ti-pillared TS-1 (D), and Ti-MCM-36 (E).

All TS-1-based catalysts possess specific BET surface areas between 465 and 595 $m^2\ g^{-1}$. The specific BET surface area of Ti-MCM-36 (786 $m^2\ g^{-1}$) as well as its specific external surface area (629 $m^2\ g^{-1}$) are higher in comparison with those of the TS-1-based catalysts due to the different framework topology of the crystalline layers of this material (MWW *vs.* MFI). The layers of Ti-MCM-36 possess side pockets on the external surface.[30] Furthermore, the layers are more regular than those in nanosheet TS-1, because Ti-MCM-36 is formed *via* a Ti-MCM-22P layered precursor.[21] Meso-TS-1 exhibits a similar specific external surface area (239 $m^2\ g^{-1}$) to layered TS-1 and Ti-pillared TS-1 (256 $m^2\ g^{-1}$ and 239 $m^2\ g^{-1}$, respectively).

The lower total adsorption capacity of Ti-pillared TS-1 (V_{total} 0.29 $cm^3\ g^{-1}$) in comparison with those of pillared TS-1 and Ti-MCM-36 (V_{total} 0.46 and 0.44 $cm^3\ g^{-1}$) can be explained by the formation of thicker pillars when a mixture of TEOS and TBOTi is used instead of pure TEOS for the pillaring procedure.[25]

The obtained pore width distribution (PWD) for meso-TS-1 clearly reflects the size (diameter 20 nm) of the carbon black pearls utilized for secondary templating (Fig. 4). The interlamellar porous structure of the lamellar catalysts belongs to the lower mesopore region (2–10 nm; *vide supra*). In order to gain information on the porous structure of the lamellar catalysts, low-pressure argon adsorption was conducted.[31] The PWD derived from argon adsorption using the NLDFT method shows two distinct pore widths (Fig. 5). A maximum of the PWD curve centered at 0.58 nm corresponds to the width of micropores present in the crystalline layers (shown for Ti-MCM-36 and Ti-pillared TS-1 in the ESI,† Fig. S2). The second maximum between 2 and 3 nm reflects the interlayer distance. This result is consistent with the interlayer distance derived from the diffraction patterns (the position of the first diffraction line,[30] Fig. 2). The

Open Access Article. Published on 01 August 2016. Downloaded on 8/2/2025 8:34:17 AM.
This article is licensed under a Creative Commons Attribution-NonCommercial 3.0 Unported Licence.

Table 1 Specific BET surface area S_{BET}, external surface area S_{ext}, micropore volume V_{micro} and total pore volume V_{total} as determined from nitrogen sorption analysis as well as Ti-content expressed as the molar ratio n_{Si}/n_{Ti} of the TS-1-based catalysts and Ti-MCM-36

Titanosilicate	S_{BET}/m^2 g^{-1}	S_{ext}/m^2 g^{-1}	V_{micro}/cm^3 g^{-1}	V_{total}/cm^3 g^{-1}	n_{Si}/n_{Ti}	d_{meso}[a]/nm
TS-1	449	95	0.16	0.21	31	n.d.[b]
Meso-TS-1	465	239	0.10	0.34	38	20.0
Layered TS-1	508	256	0.12	0.48	41	3.0[c]
Pillared TS-1	595	384	0.09	0.46	93	2.8
Ti-pillared TS-1	480	239	0.11	0.29	23	3.0
Ti-MCM-36	786	629	0.07	0.44	57	2.2

[a] The value of d_{meso} represents the maximum of the PWD in the mesopore region, presented in Fig. 5 and 6. [b] n.d.: not determined. [c] Interparticle space.

nature and coordination of the Ti-species were investigated using DR-UV-vis spectroscopy.

In the upper part of Fig. 6, the spectra of the lamellar TS-1 catalysts, *i.e.*, layered, pillared and Ti-pillared TS-1, are displayed. The main feature in these spectra is a band centered around 210 nm. This band is characteristic of an O(2p) → Ti(3d) charge transfer transition, and is generally assigned to isolated, tetrahedrally coordinated $Ti(OSi)_4$ species in hydrophobic zeolite frameworks.[32]

The spectrum of Ti-pillared TS-1 (Fig. 6) also exhibits a shoulder at approximately 260–290 nm. This absorption results from the presence of pentahedrally or octahedrally coordinated $Ti(OH)(OSi)_3(H_2O)$ and $Ti(OH)_2(OSi)_2(H_2O)_2$ species,[33] located in the amorphous pillars or on the surface of the crystalline layers. Similar spectra were observed by Přech *et al.*[34] upon impregnation of deboronated borosilicate zeolites with TBOTi solution. The decrease in the intensity of the band at 210 nm observed for pillared TS-1 with respect to layered TS-1 can be attributed to the dilution of the titanosilicate phase by the silica pillars. A higher band intensity for Ti-pillared TS-1 with respect to layered and pillared TS-1 results from post-synthesis addition of titanium during the pillaring.

In the spectrum of Ti-MCM-36, a broader band centered around 225 nm is found. The red shift of the absorption maximum suggests the simultaneous presence of tetrahedral tripodal $Ti(OSi)_3OH$ and loosely coordinated tetrapodal $Ti(OSi)_4$ species in Ti-MCM-36. The presence of these Ti-species is typical for titanosilicates with **MWW** topology.[19]

In addition, the broad line width at half maximum of the band points to the presence of pentahedrally or octahedrally coordinated $Ti(OH)(OSi)_3(H_2O)$ and $Ti(OH)_2(OSi)_2(H_2O)_2$ species.

For meso-TS-1, a band with the maximum at around 210 nm is observed together with a weak absorption centered at *ca.* 320 nm. The latter observation is indicative of the presence of an anatase-like TiO_2 phase containing Ti–O–Ti species, typically absorbing at 330 nm.

3.2 Epoxidation of methyl oleate with H_2O_2

For the TS-1-based catalysts except pillared TS-1 and Ti-pillared TS-1, both conversion of methyl oleate (MO) and conversion of H_2O_2 rise rapidly (up to X_{MO} = 92% and $X_{H_2O_2}$ = 61%) within the first 5 h of the experiment (Fig. 7).

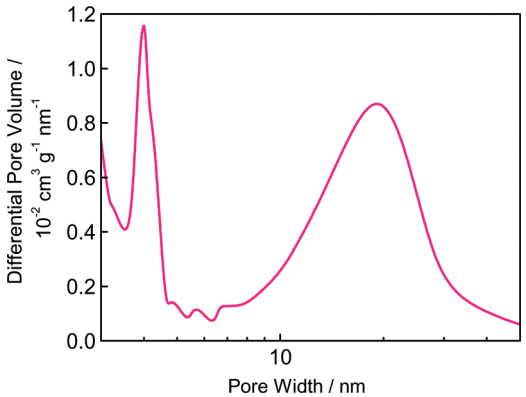

Fig. 4 BJH pore width distribution of meso-TS-1.

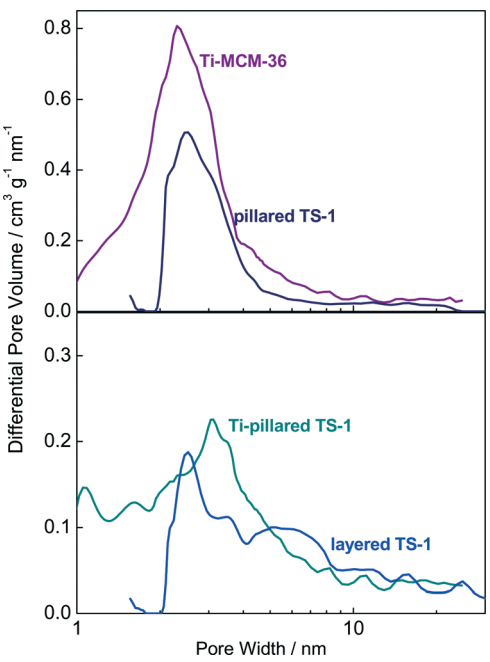

Fig. 5 NLDFT pore width distribution of Ti-MCM-36, pillared TS-1, Ti-pillared TS-1, and layered TS-1.

This journal is © The Royal Society of Chemistry 2016

Open Access Article. Published on 01 August 2016. Downloaded on 8/2/2025 8:34:17 AM.
This article is licensed under a Creative Commons Attribution-NonCommercial 3.0 Unported Licence.

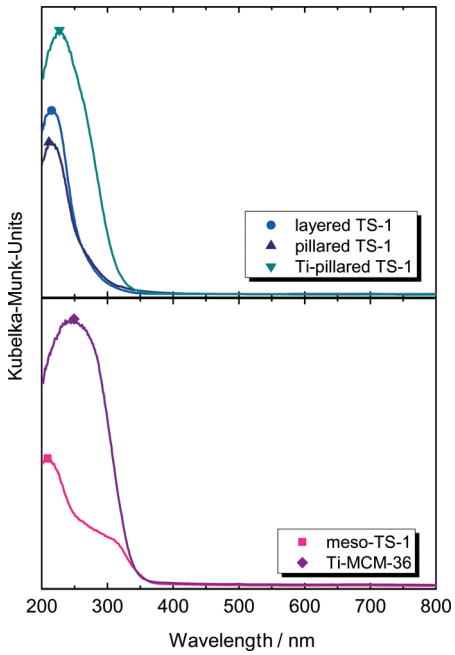

Fig. 6 DR-UV-vis spectra of the TS-1-based catalysts layered TS-1, pillared TS-1, Ti-pillared TS-1, meso-TS-1, and Ti-MCM-36.

Furthermore, the conversion increases only slightly, *e.g.*, from X_{MO} = 92% to 94%, $X_{H_2O_2}$ = 61% to 74% for layered TS-1. Among all TS-1-based catalysts, except the conventional TS-1 itself, the highest MO conversion after 5 h is achieved using layered TS-1 ($X_{MO,5h}$ = 92%) and meso-TS-1 ($X_{MO,5h}$ = 76%).

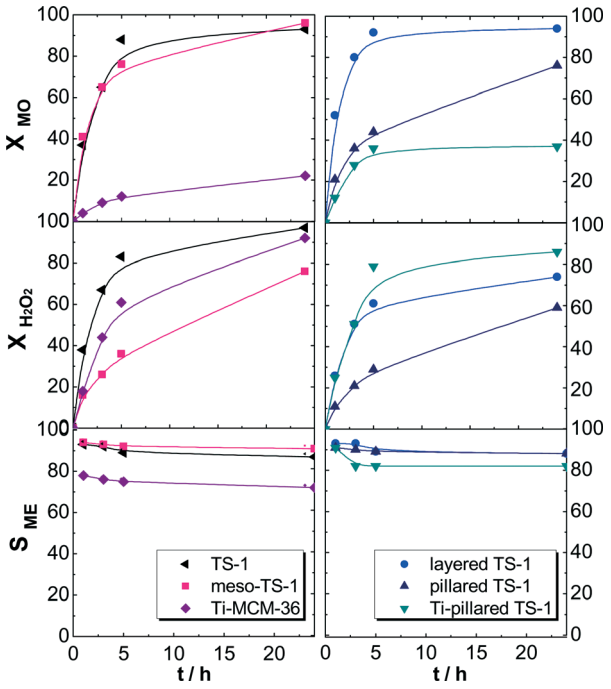

Fig. 7 Conversion of methyl oleate X_{MO}, conversion of hydrogen peroxide $X_{H_2O_2}$ and epoxide selectivity S_{ME} as a function of reaction time in the epoxidation of methyl oleate over different titanosilicate catalysts ($V_{acetonitrile}$ = 10 cm^3, c_{MO} = 0.03 mol L^{-1}, $(n_{H_2O_2}/n_{MO})$ = 5 mol mol^{-1}, m_{cat} = 150 mg, T = 50 °C).

Since both catalysts possess comparable Ti-content (layered TS-1: n_{Si}/n_{Ti} = 41 *vs.* meso-TS-1: n_{Si}/n_{Ti} = 38), specific BET surface area and external surface area (*cf.* Table 1), the structural features may account for the different activity. Sponge-like particles of meso-TS-1 are larger in size (approx. 1 μm) and denser than those of layered TS-1 (0.4 μm) (Fig. 3). The difference in the specific total pore volume (0.34 *vs.* 0.48 cm^3 g^{-1}) confirms this statement. Furthermore, it should be taken into account that mesopores in the core of the meso-TS-1 crystals (being formed by removal of the carbon black pearls) might be accessible only through the micropores.

In addition, the lower conversion of meso-TS-1 over layered TS-1 may also result from a difference in the types of accessible active Ti-sites (as revealed by DR-UV-vis spectroscopy, *vide supra*) or a lower active site density within the mesopores in meso-TS-1 with respect to the external surface of layered TS-1. In contrast to the results achieved by Přech and co-workers[25] for the epoxidation of cyclooctene with H_2O_2, the conversion of methyl oleate over pillared TS-1 ($X_{MO,5h}$ = 44%) is much lower compared to that over layered TS-1 ($X_{MO,5h}$ = 92%). This can be attributed to a lower Ti-content of the former. Relating the conversion of methyl oleate to the number of Ti-sites in layered TS-1 and pillared TS-1, a comparable activity per Ti-sites for the two catalysts results (4.64 mol mol^{-1} *vs.* 4.68 mol mol^{-1}). Although pillaring leads to expansion of the interlayer distance as well as more open reaction space (which is expected to improve accessibility of the active Ti-sites), the accessibility of the active sites for the MO molecules is not strongly different. Probably, this is due to the high steric demand of the methyl oleate molecules (high molecular weight, long carbon chain, *cis*-conformation of the internal double bond). This is supported by the fact that the conversion of methyl oleate over pillared TS-1 increases further between 5 and 24 h of reaction ($X_{MO,5h}$ = 44% *vs.* $X_{MO,24h}$ = 76%), while over layered TS-1, the methyl oleate conversion is nearly quantitative after 5 h as more active centers are accessible. Note, however, that the linkage of the pillars to the external surface of the TS-1 nanosheets leads to partial blockage of active Ti-sites. Consequently, some active Ti-sites on the external surface cannot be fully utilized for the catalytic conversion.

In order to increase the amount of Ti-sites accessible for methyl oleate, pillars comprising Ti-sites were introduced by pillaring of layered TS-1 with a mixture of TEOS and a Ti-source. The obtained catalyst Ti-pillared TS-1 is, however, less active than its counterpart with Ti-free pillars (pillared TS-1) showing a methyl oleate conversion of 36% after 5 h of reaction with an activity per Ti-sites of 1.04 mol mol^{-1}. The main disadvantage of the Ti-pillared TS-1 is the fast decomposition of H_2O_2 ($X_{H_2O_2,5h}$ = 79%). As can be seen from the DR-UV-vis spectra (Fig. 6), increasing Ti-content by pillaring with a Ti-source leads to the formation of octahedrally coordinated extra-framework Ti-species, either on the surface of the layers or within the pillars.[25] With respect to tetrahedrally coordinated Ti-species, these are supposed to be less active in the epoxidation with H_2O_2 and possibly responsible for the

Open Access Article. Published on 01 August 2016. Downloaded on 8/2/2025 8:34:17 AM.
This article is licensed under a Creative Commons Attribution-NonCommercial 3.0 Unported Licence.

higher rate of H_2O_2 decomposition.[35,36] Furthermore, compared to pillared TS-1, Ti-pillared TS-1 possesses a lower specific total pore volume in accordance with the fact that the Ti-containing pillars are broader (*vide supra*). A difference in the pillaring may lead to a decrease in the available reaction space, thus, decreasing the reaction rate. In addition, a lower amount of active tetrahedrally coordinated Ti-species on the external surface of the nanosheets could be accessible for the reactants. At the same time, a considerable amount of less active but readily accessible Ti-sites may be present in the pillars themselves.

Conventional microporous TS-1 exhibits an activity per Ti-sites of 3.37 mol mol^{-1}. While this is comparable with the activity achieved over meso-TS-1 (3.64 mol mol^{-1}), the activity of layered and pillared TS-1 (4.64 mol mol^{-1} *vs.* 4.68 mol mol^{-1}) is higher. The comparable TOF achieved over TS-1 and meso-TS-1 can be attributed to the lower particle size of the conventional catalyst (*cf.* ESI,† Fig. S12) assuming that the reaction occurs at the outer crystallite surface only.

Over all catalysts studied, the epoxide selectivity decreases steadily with reaction time due to the formation of by-products *via* consecutive reactions of the epoxide (*cf.* ref. 11).

The main by-product is methyl 9,10-dihydroxystearate (diol). The epoxide selectivity does not noticeably depend on the structural features of the catalysts, since it is comparable for the conventional TS-1, meso-TS-1, layered TS-1, as well as pillared TS-1 ($S_{ME,5h}$ = 89–92%).

Only for Ti-pillared TS-1, a lower epoxide selectivity ($S_{ME,5h}$ = 82%) is observed. This can be attributed to the presence of a larger density of octahedrally coordinated Ti-species in Ti-pillared TS-1 which facilitate consecutive reactions. Ti–OH groups in "TiO_6" species can act as acid sites on the catalyst surface[37] which may catalyze the ring opening of the epoxide to form the corresponding diol. Moreover, less available reaction space may be accessible between the layers hindering the removal of epoxide molecules from the catalyst surface before undergoing consecutive reactions. However, since Ti(IV)-species are also reported to be slightly acidic,[38,39] it is more likely that a longer residence time of the epoxide within the catalyst leads to the formation of the diol.

Based on a previous study,[11] a fivefold excess of H_2O_2 with respect to methyl oleate was used in this work. At lower molar ratios of H_2O_2 to methyl oleate (1 : 1, 2 : 1 and 3 : 1), the maximum conversion over conventional TS-1 does not exceed 65%, since H_2O_2 is completely converted within the first hours of the reaction. Furthermore, it is reported for the epoxidation of methyl oleate over Ti-MCM-41 that H_2O_2 can be more efficiently utilized when added dropwise to the reaction solution.[40] Dropwise addition of H_2O_2 in the epoxidation of methyl oleate over conventional TS-1 does not result in a higher H_2O_2 efficiency and leads to a 15% lower conversion of methyl oleate at a comparable epoxide selectivity. Thus, the conversion of hydrogen peroxide occurs by two routes (Fig. 7): the effective epoxidation of methyl oleate and the unproductive decomposition. Both reactions occur *via* formation of the Ti–hydroperoxo complex on tetrahedrally coordinated Ti(IV)-sites stabilized by a protic molecule such as methanol or water.[41] The five-membered-ring structure in this complex is believed to be the active intermediate in oxidative conversions over TS-1 with H_2O_2 as the oxidizing agent.[3,41,42] However, the formation of the Ti–OOH species narrows the effective size of the micropores.[42] In addition, the molecular size of methyl oleate is reported to be 0.5 nm × 0.5 nm × 2.5 nm,[43] while the pore width of TS-1 micropores is approx. 0.53 nm.

Hence, the epoxidation most likely takes place on the external surface of microporous TS-1 and to some extent on Ti-sites located in micropores close to the crystal external surface. In contrast to the fact that the accessibility of the zeolitic pores for the bulky methyl oleate is hindered, the active Ti–OOH intermediate can be formed inside the channels of TS-1.[42] Due to the constraints mentioned above, these species are not accessible for the bulky substrate molecules, thus, result in unproductive conversion of H_2O_2. This is evident from the methyl oleate conversion over TS-1 after 5 h which amounts to 88% at a H_2O_2 conversion of 83%. Thus, an H_2O_2 efficiency of only 18% is observed leading to the conclusion that the vast majority of H_2O_2 is converted by unproductive decomposition.

Among all catalysts studied, H_2O_2 is most efficiently used over meso-TS-1. After 5 h of reaction, an H_2O_2 efficiency of 39% is observed. The high H_2O_2 efficiency achieved over this catalyst is unexpected, since in this catalyst, crystalline TiO_2 in the anatase modification is present (*cf.* section 3.1) which is known to decompose H_2O_2.[36,41] Note, however, that the H_2O_2 efficiency observed in the epoxidation of methyl oleate is generally lower than that achieved when converting olefins with lower molecular sizes such as cyclohexene. For the latter case, H_2O_2 efficiencies of up to 75% can be reached.[44] The lower H_2O_2 efficiency for methyl oleate epoxidation is, therefore, most likely due to the bulky methyl oleate molecules which do not reach all active Ti-sites. These are, however, accessible for H_2O_2 resulting in more distinct decomposition.

For both layered and pillared TS-1, the H_2O_2 efficiency is comparable, *i.e.*, around 27% and 28%, respectively. The unproductive H_2O_2 conversion is most pronounced for Ti-pillared TS-1 over which methyl oleate conversion after 5 h reaches only 36%, whereas H_2O_2 conversion amounts to 79%, corresponding to an H_2O_2 efficiency of 8%. Besides the structural properties of the titanosilicate catalysts, the unproductive conversion of H_2O_2 can furthermore be related to the nature of the present and accessible Ti-species. Octahedrally coordinated Ti-species can decompose H_2O_2 resulting in the low H_2O_2 efficiency over Ti-pillared TS-1.[36,41]

Ti-MCM-36 shows the lowest catalytic activity (0.82 mol mol^{-1}), epoxide selectivity ($S_{ME,5h}$ = 75%) and H_2O_2 efficiency ($E_{H_2O_2,5h}$ = 3%) among all catalysts studied. Based on the results of DR-UV-vis spectroscopy, Ti-MCM-36 mainly possesses octahedrally coordinated Ti-species which are believed to be only slightly active for the epoxidation of olefins with H_2O_2.[36,41,45] Swelling/pillaring during synthesis of Ti-MCM-36 is expected to generate a large number of weakly acidic

 This journal is © The Royal Society of Chemistry 2016

Open Access Article. Published on 01 August 2016. Downloaded on 8/2/2025 8:34:17 AM.
This article is licensed under a Creative Commons Attribution-NonCommercial 3.0 Unported Licence.

silanol groups. The low H_2O_2 efficiency is, thus, a combined result of conversion over the octahedrally coordinated Ti-species as well as the silanol groups both causing unproductive H_2O_2 decomposition. In addition, the presence of silanol groups results in a more hydrophilic surface promoting the adsorption of polar products, *e.g.*, the epoxide. As a consequence, the epoxide can be further converted by acid-catalyzed hydrolysis to the diol. In fact, the diol is the predominant by-product over Ti-MCM-36 formed with a selectivity of 17%.

3.3 Reusability and regeneration of meso-TS-1, layered TS-1 and pillared TS-1

It was shown in an earlier work[11] that deactivation of conventional TS-1 during epoxidation of methyl oleate with aqueous H_2O_2 occurs due to blocking of the active Ti-sites on the outer crystal surface by organic deposits. However, for conventional TS-1, these deposits can be completely removed by calcination in air at 400 °C leading to a fully restored catalytic activity.[11]

In order to examine which compounds lead to deactivation, the conventional TS-1 catalyst (after the 2nd reuse) was extracted with tetrachloromethane and dichloromethane (see the ESI†). Electrospray ionization-mass spectrometry analysis of the extracts shows that oligomers originating from the ring-opening product of the epoxide lead to the observed deactivation (*cf.* ESI,† Fig. S13).

The most promising TS-1-based catalysts, meso-TS-1, layered TS-1 as well as pillared TS-1, were reused twice. The conversion of methyl oleate and H_2O_2 as well as the selectivity for the epoxide (ME) are shown as a function of reaction time for the reused catalysts in Fig. S6.†

For all catalysts, the activities after the 1st reuse are significantly lower compared to those of the fresh catalysts (meso-TS-1: active site-related catalytic activity, fresh = 3.64 mol mol^{-1} *vs.* 1st reuse = 1.30 mol mol^{-1}; layered TS-1: fresh = 4.64 mol mol^{-1} *vs.* 1st reuse = 1.87 mol mol^{-1}; pillared TS-1: fresh = 4.68 mol mol^{-1} *vs.* 1st reuse = 1.72 mol mol^{-1}). For layered and pillared TS-1, the activity remains unchanged during the 2nd reuse. In contrast, the activity of meso-TS-1 decreases further (0.93 mol mol^{-1}) when reused for the second time. A similar trend is also observed for the H_2O_2 efficiency, while the epoxide selectivity is comparable throughout all three consecutive catalytic experiments. A comparable H_2O_2 efficiency is observed over layered and pillared TS-1 during the 1st and 2nd reuse (layered TS-1: $E_{H_2O_2,5h}$ fresh 27%, 1st/2nd reuse 21%; pillared TS-1: $E_{H_2O_2,5h}$ fresh 27%, 1st/2nd reuse 10%). The drop in H_2O_2 efficiency is most pronounced for pillared TS-1. Over meso-TS-1, the H_2O_2 efficiency decreases to 19% ($E_{H_2O_2,5h}$ fresh 39%) after the 1st reuse, but increases slightly in the 2nd reuse ($E_{H_2O_2,5h}$ 2nd reuse 27%).

All the three catalysts are stable towards leaching of active Ti-species (*cf.* ESI,† Fig. S7) under the applied reaction conditions. In addition, the structural and textural features of the regenerated catalysts, except layered TS-1, remain virtually unaffected (*cf.* ESI,† Fig. S8–11, Table S1). Since no structural changes are observed for layered TS-1, the results from N_2-sorption indicate that the layers are partially connected to each other after regeneration, leading to a lower specific BET surface area, lower external surface area as well as lower total pore volume (*cf.* ESI,† Table S1).

4. Conclusions

TS-1-based catalysts possessing different structural features with increased accessibility of the active Ti-sites were studied in the liquid-phase epoxidation of methyl oleate with H_2O_2. In comparison with a conventional, microporous TS-1 and among all TS-1-based catalysts investigated in this study, the highest conversion of methyl oleate of 92% (amount of methyl oleate converted after 5 h per number of Ti-sites of 4.64 mol mol^{-1}) at an epoxide selectivity of 89% after 5 h of reaction is observed over layered TS-1. This clearly shows that an improved accessibility of the Ti-sites results in a higher catalytic activity with respect to a conventional, merely microporous TS-1 catalyst. Pillaring of the layered TS-1 to achieve pillared TS-1 and Ti-pillared TS-1 does not increase the catalytic activity. While the activity achieved for pillared TS-1 is comparable to that of layered TS-1 (4.68 mol mol^{-1}), that of Ti-pillared TS-1 containing Ti-sites within the pillars (1.04 mol mol^{-1} at an epoxide selectivity of 82%) is significantly lower. The pillaring with a Ti-source decreases the H_2O_2 efficiency due to the presence of extra-framework TiO_x species, leading to fast H_2O_2 decomposition. Both meso-TS-1 prepared by secondary templating with carbon black pearls and the conventional TS-1 are similarly active (3.64 *vs.* 3.37 mol mol^{-1}) and selective for the epoxide, while meso-TS-1 shows a much higher H_2O_2 efficiency.

Catalyst deactivation occurs due to blocking of active sites by oligomers formed by consecutive reactions of the epoxide. With the exception of layered TS-1, the catalytic activity and selectivity of pillared and meso-TS-1 can be completely recovered by calcination in air.

Ti-MCM-36 (pillared catalyst with **MWW** layers), containing mainly octahedrally coordinated Ti-species, provides the lowest activity (0.82 mol mol^{-1}), epoxide selectivity ($S_{ME,5h}$ = 75%) and H_2O_2 efficiency ($E_{H_2O_2,5h}$ = 3%). Based on the results achieved over the TS-1-based catalysts and Ti-MCM-36, it becomes apparent that tetrahedrally coordinated Ti-sites are more crucial to achieve high activity and selectivity in the epoxidation of high molecular-weight substrates with H_2O_2 than hierarchical porosity alone.

The benefit of hierarchically structured materials in heterogeneous catalysis is often attributed to an improved accessibility to the active sites and significantly enhanced mass transfer within the catalyst pore system. It is shown here that the presence of additional porosity provides a pronounced advantage for activity and stability of catalysts for the epoxidation of plant oil-derived substrates. Further studies should, however, target diffusion studies along with catalytic

Open Access Article. Published on 01 August 2016. Downloaded on 8/2/2025 8:34:17 AM.
This article is licensed under a Creative Commons Attribution-NonCommercial 3.0 Unported Licence.

experiments, especially for layered and pillared TS-1-based catalysts.

Acknowledgements

The authors are grateful to Prof. Dr. W.-D. Einicke, Institute of Chemical Technology, Universität Leipzig, for his assistance with measuring the nitrogen sorption isotherms. Thanks are also due to M.Sc. Karl Striegler, Institute of Chemical Technology, Universität Leipzig, for conducting the SEM investigations. The authors from J. Heyrovský Institute acknowledge the Czech Science Foundation (P106/12/G015) for the financial support to this research.

References

1 G. N. Vayssilov, *Catal. Rev.: Sci. Eng.*, 1997, **39**, 209.
2 M. G. Clerici, *Top. Catal.*, 2001, **15**, 257.
3 M. G. Clerici, *Kinet. Catal.*, 2015, **56**, 450.
4 S. Park, K. M. Cho, M. H. Youn, J. G. Seo, J. C. Jung, S. H. Baeck, T. J. Kim, Y. M. Chung, S. H. Oh and I. K. Song, *Catal. Commun.*, 2008, **9**, 2485.
5 S. C. Laha and R. Kumar, *J. Catal.*, 2002, **208**, 339.
6 R. Kumar, G. C. G. Pais, B. Pandey and P. Kumar, *J. Chem. Soc., Chem. Commun.*, 1995, 1315, DOI: 10.1039/C39950001315.
7 U. Biermann, U. Bornscheuer, M. A. R. Meier, J. O. Metzger and H. J. Schafer, *Angew. Chem., Int. Ed.*, 2011, **50**, 3854.
8 A. Campanella, E. Rustoy, A. Baldessari and M. A. Baltanas, *Bioresour. Technol.*, 2010, **101**, 245.
9 M. Galia, L. M. de Espinosa, J. C. Ronda, G. Lligadas and V. Cadiz, *Eur. J. Lipid Sci. Technol.*, 2010, **112**, 87.
10 D. Kubička, I. Kubičková and J. Čejka, *Catal. Rev.: Sci. Eng.*, 2013, **55**, 1.
11 N. Wilde, C. Worch, W. Suprun and R. Gläser, *Microporous Mesoporous Mater.*, 2012, **164**, 182.
12 N. Wilde, M. Pelz, S. G. Gebhardt and R. Gläser, *Green Chem.*, 2015, **17**, 3378.
13 J. Přech and J. Čejka, *Catal. Today*, 2015, DOI: 10.1016/j.cattod.2015.09.036.
14 M. V. Opanasenko, W. J. Roth and J. Čejka, *Catal. Sci. Technol.*, 2016, **6**, 2467.
15 W. J. Roth, P. Nachtigall, R. E. Morris and J. Čejka, *Chem. Rev.*, 2014, **114**, 4807.
16 A. Corma, U. Diaz, M. E. Domine and V. Fornes, *Chem. Commun.*, 2000, 137, DOI: 10.1039/a908748f.
17 A. Corma, M. J. Diaz-Cabanas, M. E. Domine and F. Rey, *Chem. Commun.*, 2000, 1725, DOI: 10.1039/B004203j.
18 P. Wu, T. Tatsumi, T. Komatsu and T. Yashima, *J. Catal.*, 2001, **202**, 245.
19 P. Wu, T. Tatsumi, T. Komatsu and T. Yashima, *J. Phys. Chem. B*, 2001, **105**, 2897.
20 W. Fan, P. Wu, S. Namba and T. Tatsumi, *Angew. Chem.*, 2004, **116**, 238.
21 S. Y. Kim, H. J. Ban and W. S. Ahn, *Catal. Lett.*, 2007, **113**, 160.
22 L. Wang, Y. Wang, Y. Liu, H. Wu, X. Li, M. He and P. Wu, *J. Mater. Chem.*, 2009, **19**, 8594.
23 K. Na, C. Jo, J. Kim, W.-S. Ahn and R. Ryoo, *ACS Catal.*, 2011, **1**, 901.
24 M. Choi, K. Na, J. Kim, Y. Sakamoto, O. Terasaki and R. Ryoo, *Nature*, 2009, **461**, 246.
25 J. Přech, P. Eliasova, D. Aldhayan and M. Kubů, *Catal. Today*, 2015, **243**, 134.
26 I. Schmidt, A. Krogh, K. Wienberg, A. Carlsson, M. Brorson and C. J. H. Jacobsen, *Chem. Commun.*, 2000, 2157.
27 M. Taramasso, G. Perego and B. Notari, in *Verified Syntheses of Zeolitic Materials*, ed. H. Robson, Elsevier Science, Amsterdam, 2001, pp. 207–208, DOI: 10.1016/B978-044450703-7/50164-2.
28 B. C. Lippens and J. H. de Boer, *J. Catal.*, 1965, **4**, 319.
29 E. P. Barrett, L. G. Joyner and P. P. Halenda, *J. Am. Chem. Soc.*, 1951, **73**, 373.
30 W. J. Roth, C. T. Kresge, J. C. Vartuli, M. E. Leonowicz, A. S. Fung and S. B. McCullen, in *Studies in Surface Science and Catalysis*, ed. H. G. K. I. K. H. K. Beyer and J. B. Nagy, Elsevier, 1995, vol. 94, pp. 301–308.
31 S. Lowell, J. E. Shields, M. A. Thomas and M. Thommes, *Characterization of Porous Solids and Powders: Surface Area*, Pore Size and Density Springer, Dordrecht, 2006.
32 A. Zecchina, S. Bordiga, C. Lamberti, G. Ricchiardi, C. Lamberti, G. Ricchiardi, D. Scarano, G. Petrini, G. Leofanti and M. Mantegazza, *Catal. Today*, 1996, **32**, 97.
33 P. Ratnasamy, V. N. Shetti, P. Manikandan and D. Srinivas, *J. Catal.*, 2003, **216**, 461.
34 J. Přech, D. Vitvarova, L. Lupinkova, M. Kubů and J. Čejka, *Microporous Mesoporous Mater.*, 2015, **212**, 28.
35 F. Bonino, A. Damin, G. Ricchiardi, M. Ricci, G. Spano, R. D'Aloisio, A. Zecchina, C. Lamberti, C. Prestipino and S. Bordiga, *J. Phys. Chem. B*, 2004, **108**, 3573.
36 T. Tatsumi, in *Modern Heterogeneous Oxidation Catalysis*, Wiley-VCH Verlag GmbH & Co. KGaA, 2009, ch. 4, pp. 125–155, DOI: 10.1002/9783527627547.
37 G. Ricchiardi, A. de Man and J. Sauer, *Phys. Chem. Chem. Phys.*, 2000, **2**, 2195.
38 J. M. Fraile, J. I. García, J. A. Mayoral, L. Salvatella, E. Vispe, D. R. Brown and G. Fuller, *J. Phys. Chem. B*, 2003, **107**, 519.
39 A. Bhaumik and T. Tatsumi, *J. Catal.*, 1999, **182**, 349.
40 M. Guidotti, E. Gavrilova, A. Galarneau, B. Coq, R. Psaroa and N. Ravasio, *Green Chem.*, 2011, **13**, 1806.
41 C. W. Yoon, K. F. Hirsekorn, M. L. Neidig, X. Z. Yang and T. D. Tilley, *ACS Catal.*, 2011, **1**, 1665.
42 P. Wu, T. Komatsu and T. Yashima, *J. Phys. Chem. B*, 1998, **102**, 9297.
43 L. A. Rios, P. Weckes, H. Schuster and W. F. Hoelderich, *J. Catal.*, 2005, **232**, 19.
44 J. G. Wang, L. Xu, K. Zhang, H. G. Peng, H. H. Wu, J. G. Jiang, Y. M. Liu and P. Wu, *J. Catal.*, 2012, **288**, 16.
45 M. Sasaki, Y. Sato, Y. Tsuboi, S. Inagaki and Y. Kubota, *ACS Catal.*, 2014, **4**, 2653.

 This journal is © The Royal Society of Chemistry 2016